JOC The Journal of Organic Chemistry

Article

pubs.acs.org/joc

Conformational Analysis of a Model Synthetic Prodiginine

María García-Valverde,[†] Ignacio Alfonso,[‡] David Quiñonero,*[,§] and Roberto Quesada*[,†]

[†]Departamento de Química, Facultad de Ciencias, Universidad de Burgos, 09001 Burgos, Spain

[‡]Departamento de Química Biológica y Modelización Molecular, Instituto de Química Avanzada de Cataluña (IQAC−CSIC), Jordi Girona, 18-26, E-08034, Barcelona, Spain

[§]Departament de Química, Universitat de les Illes Balears, 07122 Palma de Mallorca, Spain

Supporting Information

ABSTRACT: A conformational analysis of a synthetic model prodiginine was carried out. In solution this compound showed a strong preference for the β conformation, in which all the heterocycles are mutually cis. This conformation provided an ideal alignment of the three N−H groups for interacting with anions when the molecule is protonated. A different conformation was also detected in d_6-DMSO for the mesylate salt, assigned to the α conformation, in which the C ring is engaged in an intramolecular hydrogen bond with the OMe group. The formation of a homodimer was observed in concentrated $CDCl_3$ solutions of the neutral free base form of this prodiginine derivative. DFT calculations and the solid state structures of the hydrochloric and methanesulfonic acid salts were in good agreement with the results observed in solution. A complete study of the relative energies of different tautomers, isomers, and supramolecular complexes supported the preference for the β conformation both in water and in the gas phase.

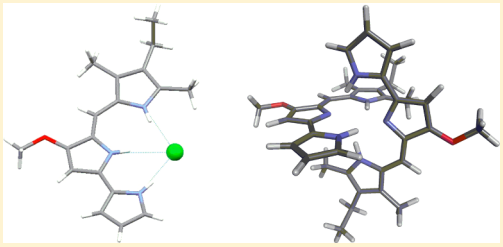

INTRODUCTION

The prodiginines are a family of natural compounds characterized by a 4-methoxy bipyrrol moiety linked to a variety of alkyl substituted pyrroles, prodigiosin **2** being the most representative example.[1] These compounds have been extensively studied for their intriguing pharmacological properties.[2−8] Inmunosuppressive, antibiotic, antimalarial and anticancer activities have all been identified for these compounds. Some of these compounds have shown potential in the clinic, and the synthetic prodiginine analog obatoclax **3** has completed phase II clinical trials for the treatment of small cell lung cancer and is engaged in multiple clinical trials for the treatment of other cancer conditions.[9] Despite their apparent structural simplicity, the prodiginines potentially present multiple tautomeric and rotameric forms. Indeed, different representations can be found in the literature. The prodiginines can exist as free bases or protonated species and both can interact with anions through hydrogen bonds and function as ionophores.[10] Most reported works deal with the synthesis and structural elucidation of natural prodiginines and synthetic analogs, paying little attention to the conformational analysis of these molecules.[11−14] Theoretical studies of this class of compounds are also surprisingly scarce.[15,16] The molecular target(s) and mode of action of prodiginines have not been established as yet.[17−19] However, different conformations should have different binding affinities for a given substrate. In this regard, there are very few studies concerning the conformational analysis of these derivatives and their supramolecular complexes. In this work, we addressed this goal by studying the model synthetic prodiginine **1** using NMR and DFT calculations of both the free base form and different supramolecular complexes with anions as well as in the solid state (Figure 1).

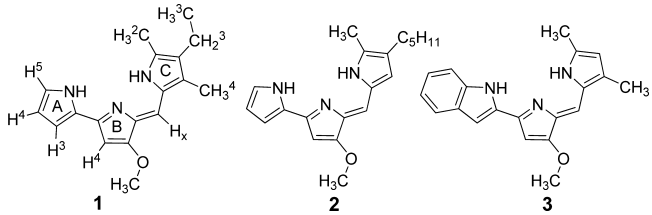

Figure 1. Structures of synthetic prodiginine **1**, prodigiosin **2**, and obatoclax **3**.

RESULTS AND DISCUSSION

Compound **1** was prepared by acid catalyzed condensation of 4-methoxy-2,2′-bipyrrol-5-carbaldehyde and 2,4-dimethyl-3-ethyl-1H-pyrrole. Using HCl and $MeSO_3H$ as acids, the corresponding protonated salts **1**·HCl and **1**·$MeSO_3H$ were obtained as dark red crystalline solids. The solid state structures of these salts were determined by X-ray diffraction (Figure 2). In both cases, the receptor adopted a conformation with the three NH groups engaged in hydrogen bonds pointing toward the anions (N···Cl distances = 3.19−3.23 Å, N−H···Cl angles = 164.1−169.7° in **1**·HCl; N···O distances = 2.80−3.29 Å, N−H···O angles = 143.4−75.3° in **1**·$MeSO_3H$). We named this conformation as β conformation.[10] The tripyrrolic structure

Received: May 28, 2012
Published: July 19, 2012

   dx.doi.org/10.1021/jo301008c | J. Org. Chem. 2012, 77, 6538−6544

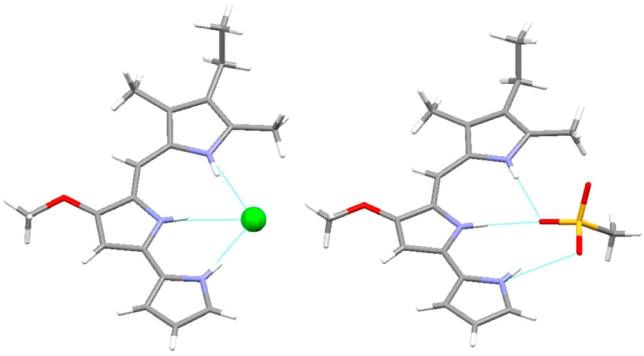

Figure 2. X-ray structures of **1**·HCl (left) and **1**·$MeSO_3H$ (right).

was found to be essentially flat reflecting the high conjugation of the molecule. All the C−C bonds connecting the methine linkage displayed similar distances (around 1.38 Å on average). The C−C bond connecting the two pyrrole rings of the bipyrrole moiety is also significantly shorter than a single bond.

The complete assignment of ^1H and ^{13}C signals for **1**·HCl was performed by 2D NMR experiments ($CDCl_3$) COSY, NOESY, HMBC, HSQC (see Supporting Information for details). All the spectroscopic data were consistent with the receptor adopting a β conformation, in agreement with the structure found in the solid state. A similar study was repeated in the more polar solvent d_6-DMSO, with the same result. We next investigated the mesylate salt of **1**·$MeSO_3H$. Mesylate is a poorer hydrogen bond acceptor compared with chloride and it is used as counterion for drug formulation of the related synthetic prodiginines.[9] The ^1H NMR in $CDCl_3$ of **1**·$MeSO_3H$ is similar to that found for **1**·HCl, and this salt showed a β conformation in this solvent. Nevertheless, when the ^1H NMR was recorded in d_6-DMSO, two different set of signals corresponding to two different conformations could be observed (Figure S28, Supporting Information). The major isomer corresponded to the β conformation and the minor isomer corresponded to a conformation in which the C ring is engaged in an intramolecular hydrogen bond with the OMe group. We named this conformation as α. Similar situation was reported by Rizzo and colleagues for 4-benzyloxy substituted synthetic prodiginine.[20] In that study, those authors found a similar mixture of isomers in $CDCl_3$. Addition of chloride (as tetrabutylammonium salt) to a solution of **1**·$MeSO_3H$ in d_6-DMSO resulted in the quantitative replacement of the mesylate anion by chloride after 1 equivalent of TBACl is added, leading to a ^1H NMR indistinguishable from **1**·HCl, that is with only the β conformation present (see Figure S39, S40, Supporting Information). An apparent association constant could be calculated from this titration experiment at 1520 (±177) M^{-1}.[21] Anion exchange can also be observed when a dichloromethane solution of **1**·$MeSO_3H$ is treated with diluted aqueous HCl, leading to a quantitative formation of **1**·HCl. From these experiments it is clear that the nature of both the solvent and the counterions can influence the conformation of the prodiginine. This result also underscores that it is likely that in physiological media the mesylate anion is replaced by chloride.

We next investigated the neutral free base form of the prodiginine **1**. 2D NMR experiments were in agreement with a β form of the receptor. Interestingly, the NOESY experiment also revealed important structural information. NOESY couplings between Hx and CH_{3C}[2] supported the formation of a homodimer in solution (Figure S7, Supporting Information). This type of dimer had been previously observed in the solid state,[2,22] but no evidence of its existence in solution had been reported. NH signals are very broad at room temperature in $CDCl_3$. Nevertheless, by acquiring the spectra upon cooling to −50 °C sharp signals can be observed (Figure S8, Supporting Information). The lack of long distance correlations with H_B[4] suggested that the favored tautomeric form is the B-azafulvene. Dilution studies were performed for **1** in $CDCl_3$ and shifts of all pyrrolic CH signals can be observed (Figure S42, Supporting Information). From this experiment, a dimerization constant of K_D = 361 (±22) M^{-1} could be calculated.[21] 2D NOESY experiments at low concentrations showed no intermolecular cross peaks suggesting that under these conditions the self-association of the receptor no longer takes place to a significant extend. Likewise, experiments in a more competitive solvent such as d_6-DMSO did not show any indications of dimer formation (Figure S13, Supporting Information).

Further evidence for the existence of the dimer species at higher concentrations was obtained by means of diffusion-ordered 2D ^1H NMR spectroscopy experiments (DOSY) of **1** at different concentrations in $CDCl_3$.[23] The results obtained for 2 mM and 40 mM samples of **1** using tetrakis(trimethylsilyl)-silane (TTMS, δ = 0.22 ppm) as internal reference (2 mM) are depicted in Figure 3. Both the signals of the reference and that

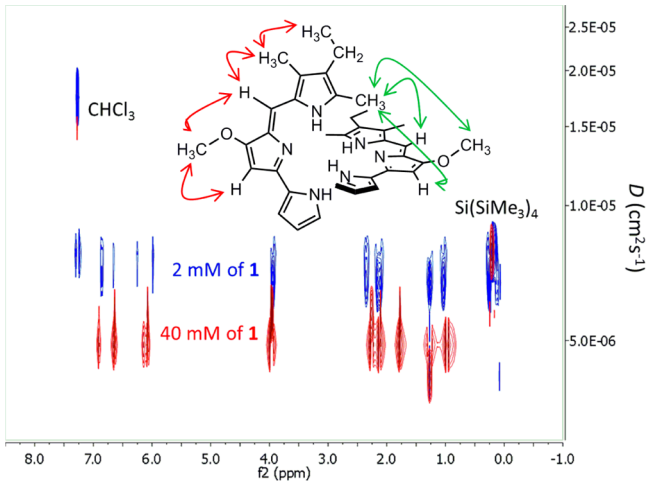

Figure 3. Superposition of the corresponding DOSY NMR spectra (500 MHz, $CDCl_3$, 298 K) showing the observed differences in the self-diffusion rates of **1** at different concentrations (2 mM blue, 40 mM red). (Inset) Proposed structure of dimer $\mathbf{1}_2$ showing the observed intra- and intermolecular NOE contacts.

of the residual solvent ($CHCl_3$) showed the same corresponding self-diffusion rates in both samples.[24] This observation ensures that the differences observed in the self-diffusion rate of the signals of **1** are not due to changes in the viscosity of the samples. The self-diffusion rates of **1** at the dissimilar concentrations were significantly different, being slower in the concentrated sample. Since the self-diffusion rate (D) is inversely proportional to the hydrodynamic radius (R_H), this observation clearly supported the self-assembly of **1** at relatively high concentrations. Moreover, the increase of the size can be estimated. For every sample, we can propose this ratio:

dx.doi.org/10.1021/jo301008c | J. Org. Chem. 2012, 77, 6538−6544

Scheme 1. Tautomers I, II and III, Isomers α and β and Rotamers γ and δ of Prodiginine 1 Considered in our Computational Study[a]

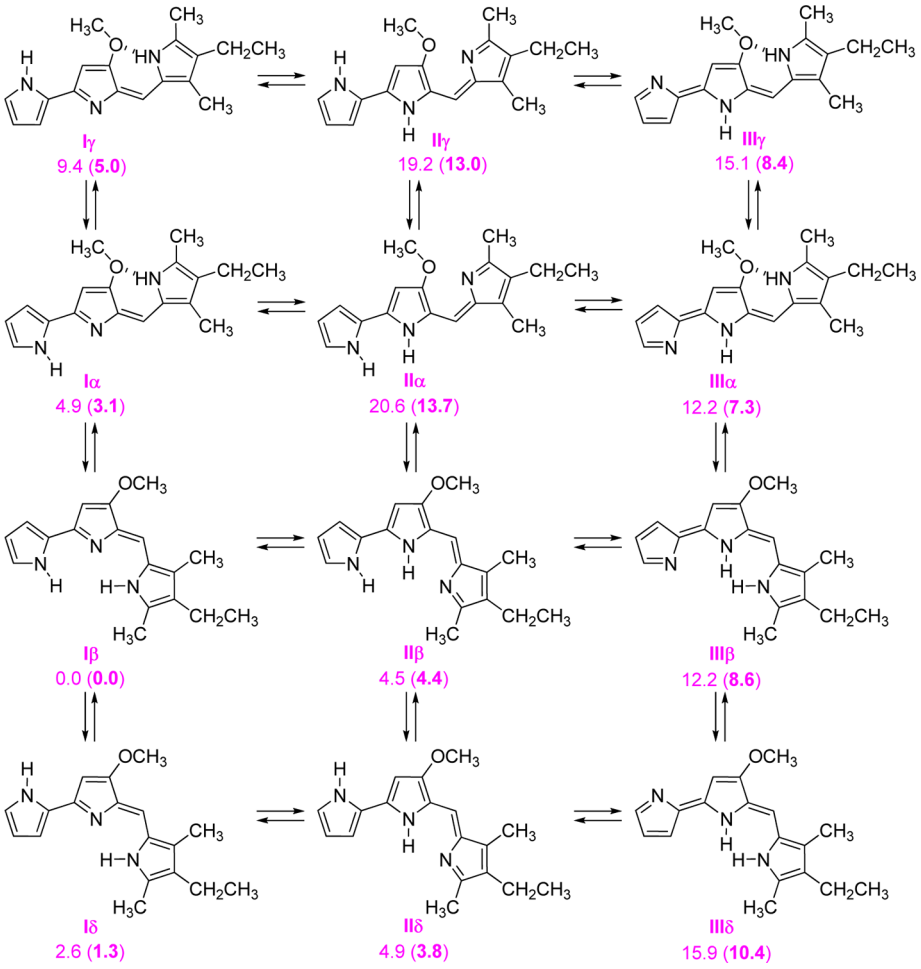

[a]Relative energies, in kcal/mol, for both gas phase and water solution (in parentheses) are shown.

$$D(\text{compound } \mathbf{1})/D(\text{reference}) = R_H(\text{reference})/R_H(\text{compound } \mathbf{1})$$

Since R_H(reference) for this compound is constant and D(reference) rendered the same value within the experimental error in the DOSY measurement of both samples, we can extract:

$$D(\text{diluted } \mathbf{1})/D(\text{concentrated } \mathbf{1}) = R_H(\text{concentrated } \mathbf{1})/R_H(\text{diluted } \mathbf{1})$$

From the DOSY experiments: D(diluted **1**) = 6.7×10^{-6} cm^2s^{-1} and D(concentrated **1**) = 4.9×10^{-6} cm^2s^{-1}, and thus:

$$R_H(\text{concentrated } \mathbf{1})/R_H(\text{diluted } \mathbf{1}) = 1.37$$

This value is in reasonably good agreement with a monomer–dimer equilibrium, whereas the theoretical increase of R_H should be 1.26 (assuming equal solvation and spherical shapes of both dimer and monomer species).

To gain a deeper understanding of the tautomeric and rotameric equilibria of prodiginine **1**, as well as to explore other solvents in which limited solubility precluded experimental investigations, such as water, DFT studies were carried out. To our knowledge this is the first exhaustive and systematical computational study dealing with such issues. The free base form of prodiginine **1** may exist in solution as a mixture of tautomers. For our study we have considered **I**, **II** and **III** (Scheme 1). These tautomers differ in the location of the unprotonated azafulvene nitrogen atom. Thus, tautomers **I**, **II** and **III** have the unprotonated azafulvene located on the B-, C- and A-rings, respectively. In addition to issues regarding different tautomers, there is even more potential for structural complexity with the prodiginine **1** because of different conformations about the methyne linkage connecting the B- and C-rings. As shown in Scheme 1, the free base of prodiginine **1** can adopt either the α-isomer or the β-isomer. The α-isomer is stabilized by a hydrogen bond between the NH proton of the C-ring and the oxygen atom of the B-ring's methoxy group. For the β-isomer, which is the conformation that is usually drawn in the literature, the three pyrrole rings are all cis to one another, with each nitrogen atom oriented toward the center of a cleft. Transformation of the two isomers α and β corresponds to a *cis*–*trans* isomerization about the double bond connecting the B- and C-rings. Two more conformations can be also considered, namely, the γ and δ isomers (Scheme 1) corresponding to the rotamers about the single bond connecting the A- and B-rings of the α and β isomers, respectively. Therefore, for every of the three tautomeric forms of **1** there are four isomers, which gives a total number of twelve different structures. This set of structures has been

dx.doi.org/10.1021/jo301008c | J. Org. Chem. 2012, 77, 6538–6544

finally considered in our computational study of the equilibria in both gas phase and solution (water) of the neutral free base form of prodiginine **1**, as depicted in Scheme 1.

The relative energies of all tautomers and conformers of **1** are gathered in Scheme 1. From the inspection of these results several conclusions can be drawn. First, gas phase and solution results predict more or less the same energy ordering of the molecular species. Second, for both gas phase and solution the lowest-energy structure corresponds to the tautomer **I** with the β conformation (**I**β), which is our energetic reference. This result is in disagreement with previous work by Cole and colleagues.[15] These authors found that, in the gas phase, the lowest-energy conformation was the **I**γ instead of the **I**β which was the one they experimentally observed, with an energy difference of only 4 kJ/mol. However our result is in excellent agreement with our 2D NMR experimental results which at the same time are in accordance with the β form of **1** and the B-azafulvene (**I**) as the favored tautomeric form. Moreover, calculations in unsubstituted parent systems also are in agreement with this result.[14] In our calculations, the **I**γ form is located 9.4 and 5.0 kcal/mol higher than **I**β in gas phase and solution, respectively. The second lowest-energy conformer is **I**δ (rotamer of **I**β) which is 2.6 and 1.3 kcal/mol higher than **I**β in gas phase and solution, respectively. From now on we will only discuss the energetic results taking into account water as the solvent since they are qualitatively the same as those in the gas phase. In general, conformers of tautomer **I** are much lower in energy than those of **II** and **III**, with the exception of **II**δ and **II**β, that are more favored than **I**γ by 1.2 and 0.6 kcal/mol. The order of relative energies of **1** was found to be **I**β < **I**δ < **I**α < **II**δ < **II**β < **I**γ for those conformers within 5.0 kcal/mol from **I**β. Moreover, all these conformers possess an extremely flat tripyrromethene framework, with only the methyl and methoxy hydrogens and the ethyl out of the plane. The conformers **II**α and **II**γ are the most energetic with relative energies of 13.7 and 13.0 kcal/mol, respectively. This is most likely due to the repulsive interaction between the N atom of the C-ring and the oxygen atom. Both gas phase optimized structures are not planar mainly because of the twisted bipyrrolic A and B-rings. However, planarity is obtained when solvent effects are taken into account. Other nonflat configurations, both in gas phase and solution, are found for **III**β and **III**δ a fact attributable to the repulsive interaction between the pyrrole NH atoms of B- and C-rings. The remaining tautomers, **III**γ and **III**α, are flat since now the pyrrole NH atom of C-ring is "*trans*" to the pyrrole NH atom of B-ring, establishing a hydrogen bond with the oxygen atom of the B-ring's methoxy group.

We have also computationally studied the conformers of the molecular species that resulted from protonation of the neutral compound **1**. The relative energies of all conformers of **1**H$^+$ are gathered in Scheme 2. From the inspection of these results several conclusions can be drawn. First, gas phase and solution results predict more or less the same energy ordering of the molecular species with the exception of **IV**β and **IV**δ which is reversed. Second, for both gas phase and solution the lowest-energy structure corresponds to the γ-isomer, and thus it will be our energetic reference. The second lowest-energy conformer is its rotamer **IV**α which is almost isoenergetic to **IV**γ in water. The order of relative energies of **1**H$^+$ was found to be **IV**γ < **IV**α < **IV**δ < **IV**β in the gas phase and **IV**γ < **IV**α < **IV**β < **IV**δ in aqueous solution. Thus the conformation expected to bind the anion (the "all *cis*" β-isomer) is only 2.5 kcal/mol higher in energy than the γ-isomer. From the geometric point of view the

Scheme 2. Isomers α and β and Rotamers γ and δ of Protonated Prodiginine 1 Considered in our Computational Study[a]

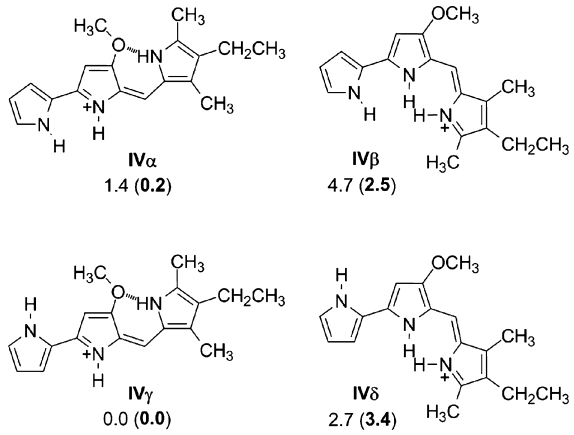

[a]Relative energies, in kcal/mol, for both gas phase and water solution (in parentheses) are shown.

isomers α, β and δ are not planar in the gas phase and in solution planarity is only observed for **IV**α. The γ-isomer is flat in both gas phase and solution.

Further energetic and optimized geometric characteristics of the complexes with mesylate and chloride anions were obtained by means of theoretical calculations. The binding energies were obtained by considering compound **1**H$^+$ in its lowest energy conformation, **IV**γ, as our reference molecule. Therefore all computed binding energies of complexes of **1**H$^+$ with mesylate and chloride anions are referred to its gamma conformation (Scheme 3).

We have systematically explored the formation of complexes of **1**H$^+$ by considering its four isomers interacting with the anions. Therefore we have computed four complexes of **1**H$^+$ for every anion. The interaction energies of these complexes are collected in Scheme 3. For every isomer it can be observed that the interaction energy of complex **1**·HCl is larger than the one of complex **1**·$MeSO_3H$ both in the gas phase, DMSO and water, in agreement with our NMR titration experimental studies of **1**·$MeSO_3H$ with TBACl in DMSO where $MeSO_3^-$ is displaced by Cl^-. Both in the gas phase and solution the β-isomer is the most favored conformation for anion binding. As expected, while **IV**α is stabilized by hydrogen bonding between B- and C-rings, the binding of the anion into the "all-*cis*" tripyrrole cleft shifts the equilibrium to favor the **IV**β isomer where each of the three NH protons point toward the bound anion. This result is also in agreement with the correlations observed in the NOESY spectra of **1**.HCl and **1**.$MeSO_3H$ in CD_3Cl (see Supporting Information). Thus, for chloride, the largest binding energy is −10.9 kcal/mol in DMSO for the β-conformation followed by the α-conformation, 2.1 kcal/mol higher in energy. For mesylate the same trend is observed, −8.9 and −7.3 kcal/mol in DMSO for its β- and α-conformations, respectively, though their energy difference is smaller, only 1.6 kcal/mol. These theoretical results would find an explanation why we experimentally observe two different conformations of **1**·$MeSO_3H$ in d_6-DMSO, but not for **1**·HCl, being the β-conformation the major isomer. Moreover, the results of ^{1}H NMR experiments suggested that the minor isomer of **1**·$MeSO_3H$ was the one with the α-conformation, and our calculations clearly support this assumption. In fact, the γ- and

dx.doi.org/10.1021/jo301008c | J. Org. Chem. 2012, 77, 6538−6544

Scheme 3. Calculated Binding Energies, in kcal/mol, for 1H$^+$ towards Mesylate and Chloride in Gas Phase, DMSO (in brackets), and Water (in parentheses)

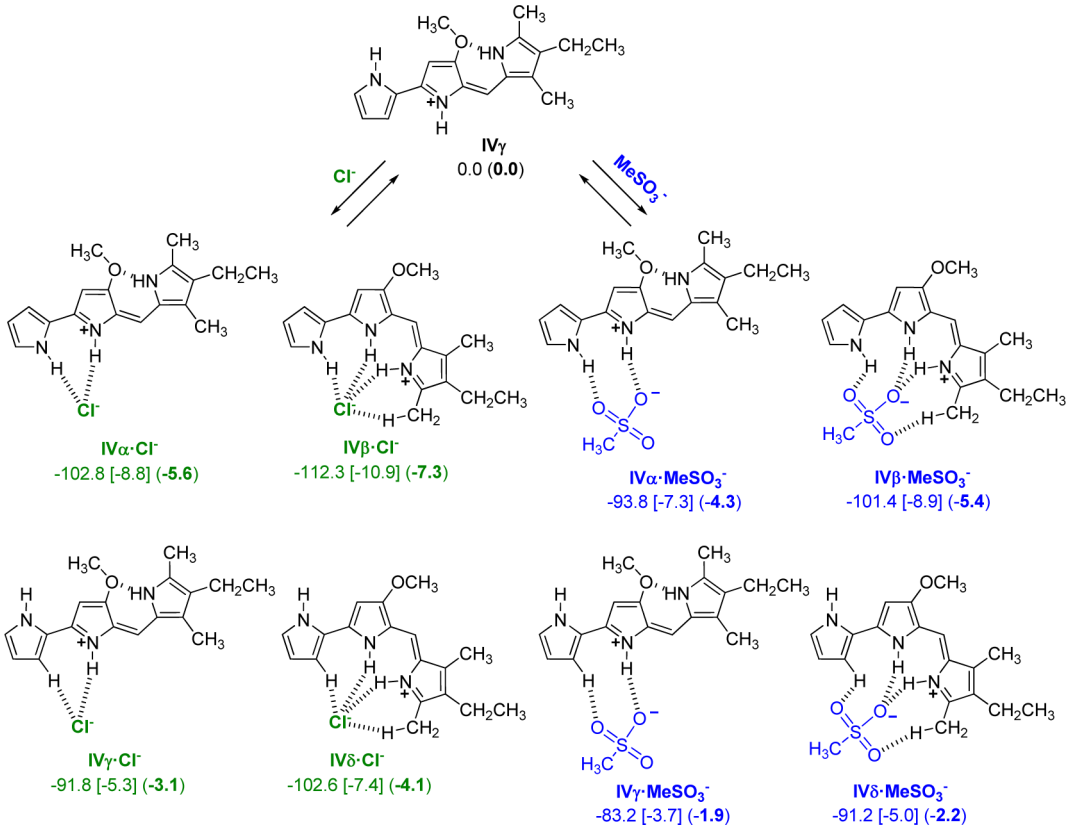

δ-isomers are 3.6 and 2.3 kcal/mol higher than the α-isomer in DMSO. The binding energy ordering for both chloride and mesylate complexes is qualitatively the same regardless of the solvent, that is, $\beta > \alpha > \delta > \gamma$.

A comparison of the optimized and experimental structures of complexes **1**·HCl and **1**·$MeSO_3H$ supported the reliability of the theoretical level used in the analysis. In Figure 4 we represent selected geometric features of the DFT solvent-free optimized complexes and their crystal structures. From the inspection of the results, first, we observe that both bond lengths and angles of the optimized and experimental structures of **1**·HCl are in excellent agreement. Second, the computed noncovalent distances between the chloride and mesylate anions and the receptor are a bit shorter than the experimental ones. This result is not surprising since in general the equilibrium distances of complexes are shorter in the gas phase than in the solid state due to packing forces and, particularly, the chloride anion participates in an additional noncovalent interaction with a CH atom (2.775 Å) of a neighboring **1**H$^+$ molecule. The experimental and computed mesylate complex show hydrogen bond angles that are a bit off which may be due to the location of the methyl group of the mesylate anion: In the crystal structure it slightly points toward the methyl group at 2-position on C-ring of **1**H$^+$ to avoid a repulsive interaction with a methyl group at 4-position on C-ring of a neighboring **1**H$^+$ cation and, at the same time establishing a nonconventional hydrogen bond with the oxygen atom of the B-ring's methoxy group of this cation. However in the computed structure there are no such interactions and the mesylate methyl group is slightly tilted toward to the A-ring.

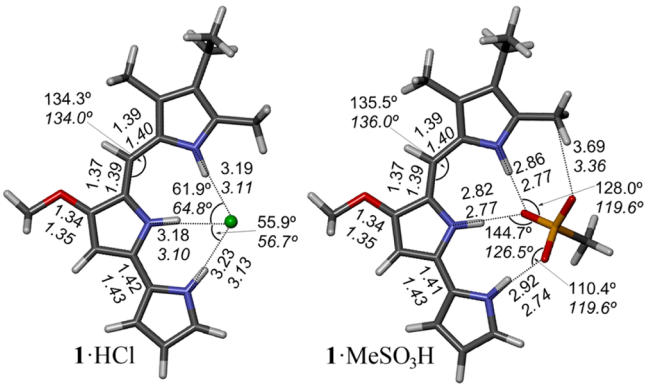

Figure 4. Comparison of the **1**·HCl (left) and **1**·$MeSO_3H$ (right) optimized gas phase geometries (italics) with the X-ray structure (plain). Distances in angstroms and angles in degrees.

■ CONCLUSION

In summary, we have studied the conformational behavior of a model synthetic prodiginine by using X-ray diffraction, NMR and DFT calculations. The conformation of this derivative is influenced by the nature of the solvent and the counterion as well as the protonation state. The most favorable conformation is the β, providing an ideal alignment of all the NH hydrogen bond donors in order to interact with the different anions, or even another molecule in the case of the neutral free base. DFT calculations largely support the results observed in solution and the solid state. A discussion of the relative energies of different conformation in other solvents such as water is provided. The present study expands the understanding of the conformational

dx.doi.org/10.1021/jo301008c | J. Org. Chem. 2012, 77, 6538−6544

behavior of an important family of compounds with potential as future drugs.

EXPERIMENTAL SECTION

General Procedures and Methods. Commercial reagents were used as received without any further purification. NMR spectra were recorded on spectrometers (FT, 300 MHz for ^{1}H; 75 MHz for ^{13}C; FT, 400 MHz for ^{1}H; 100 MHz for ^{13}C). Chemical shifts are reported in ppm with using residual solvent peak as reference, coupling constants are reported in Hz. The DOSY ^{1}H NMR experiments were performed at 500 MHz field with a z-gradient indirect probe. The DgcsteSL_cc sequence was used with 30 increments of the gradient power, while the diffusion delay was optimized for each sample to obtain a 90−95% of signal attenuation. The temperature was set to 298 K and the data acquired without spinning the sample. High resolution mass spectra (HRMS) were recorded on a magnetic sector mass spectrometer using electron impact ionization (EI). 4-methoxy-1H,1′H-2,2′-bipyrrole-5-carbaldehyde was prepared as described.[25]

(Z)-2-(2-((1H-Pyrrol-2-yl)methylene)-3-methoxy-2H-pyrrol-5-yl)-1H-pyrrole Hydrochloride **1**·HCl. 4-Methoxy-1H,1′H-2,2′-bipyrrole-5-carbaldehyde (0.1, g 0.52 mmol) was dissolved in 5 mL of methanol under an inert atmosphere. To this solution was added 141 μL (1.05 mmol) of 2,4-dimethylpyrrole followed by dropwise addition of 1 mL of 1.25 M HCl in methanol. The color changed to dark red and the mixture was stirred overnight. The solid formed was filtered off and washed with hexane and cold methanol (1 mL) yielding compound **1**·HCl (0.12 g, 70%) as a dark red crystalline solid. Mp = 249−252 °C (dec.). ^{1}HNMR ($CDCl_3$, 400 MHz): δ ppm 12.58 (br s, 1H, NH_B), 12.50 (br s, 2H, NH_A, NH_C), 7.17−7.16 (m, 1H, $H_A{}^5$), 6.99 (s, 1H, H_X), 6.85−6.83 (m, 1H, $H_A{}^3$), 6.31−6.29 (m, 1H, $H_A{}^4$), 6.04 (d, J = 1.9 Hz, 1H, $H_B{}^3$), 3.97 (s, 3H, $(OCH_3)_B{}^4$), 2.53 (s, 3H, $(CH_3)_C{}^5$), 2.39 (q, J = 7.6 Hz, 2H, $(CH_2)_C{}^4$), 2.20 (s, 3H, $(CH_3)_C{}^3$), 1.04 (t, J = 7.6 Hz, 3H, $(CH_2)_C{}^4$). ^{13}CNMR ($CDCl_3$, 100 MHz) δ ppm 165.2 (Cq), 147.4 (Cq), 146.6 (Cq), 137.7 (Cq), 128.5 (Cq), 126.2 ($CH_A{}^5$), 124.4 (Cq), 122.6 (Cq), 119.7 (Cq), 116.2 ($CH_A{}^3$), 113.2 (CH_x), 111.5 ($CH_A{}^4$), 92.7 ($CH_B{}^3$), 58.7 ($(OCH_3)_B{}^4$), 17.4 ($(CH_2)_C{}^4$), 14.8 ($(CH_3)_C{}^4$), 12.5 ($(CH_3)_C{}^5$), 10.0 ($(CH_3)_C{}^3$).

^{1}H NMR (DMSO-d_6, 400 MHz) δ ppm 12.57 (br s, 1H, NH_C), 12.38 (br s, 2H, NH_B), 12.30 (br s, 2H, NH_A), 7.41 (br s, 1H, $H_A{}^3$), 7.37 (br s, 1H, $H_A{}^5$), 7.03 (s, 1H, H_X), 6.73 (d, J = 1.2 Hz, 1H, $H_B{}^3$), 6.39−6.37 (m, 1H, $H_A{}^4$), 4.01 (s, 3H, $(OCH_3)_B{}^4$), 2.42 (s, 3H, $(CH_3)_C{}^5$), 2.38 (q, J = 7.5 Hz, 2H, $(CH_2)_C{}^4$), 2.18 (s, 3H, $(CH_3)_C{}^3$), 1.04 (t, J = 7.5 Hz, 3H, $(CH_2)_C{}^4$). ^{13}C NMR (DMSO-d_6, 100 MHz): δ166.3 (Cq), 147.7 (Cq), 147.0 (Cq), 138.1 (Cq), 128.8 (Cq), 127.4 (CH), 124.3 (Cq), 122.7 (Cq), 120.2 (Cq), 117.6 (CH), 113.3 (CH), 112.6 (CH), 94.8 (CH), 59.9 ($(OCH_3)_B{}^4$), 17.3 ($(CH_2)_C{}^4$), 15.3 ($(CH_3)_C{}^4$), 12.6 ($(CH_3)_C{}^5$), 10.1 ($(CH_3)_C{}^3$). HRMS (EI) m/z calcd for $[C_{18}H_{21}N_3O]$ 295.1679; found: 295.1685.

The analogous mesylate salt was prepared using methanesulfonic acid instead of hydrochloric acid.

^{1}H NMR ($CDCl_3$, 400 MHz) of **1**·$MeSO_3H$ δ ppm 11.89 (br s, 1H, NH_C), 11.69 (br s, 2H, NH_A, NH_B), 7.22−7.20 (m, 1H, $H_A{}^5$), 7.02 (s, 1H, H_X), 6.88 (ddd, J = 3.9, 2.6, 1.4 Hz, 1H, $H_A{}^3$), 6.34−6.32 (m, 1H, $H_A{}^4$), 6.09 (d, J = 2.0 Hz, 1H, $H_B{}^3$), 4.00 (s, 3H, $(OCH_3)_B{}^4$), 2.92 (s, 3H, CH_3SO_3), 2.55 (s, 3H, $(CH_3)_C{}^5$), 2.40 (q, J = 7.5 Hz, 2H, $(CH_2)_C{}^4$), 2.22 (s, 3H, $(CH_3)_C{}^3$), 1.05 (t, J = 7.5 Hz, 3H, $(CH_2)_C{}^4$).

^{1}HNMR (DMSO-d_6, 400 MHz) of **1**·$MeSO_3H$ δ ppm 12.22 (br s, 0.28H, $NH_{B\alpha}$), 12.03 (br s, 0.72H, $NH_{A\beta}$), 11.98 (br s, 0.28H, $NH_{A\alpha}$), 11.72 (br s, 0.72H, $NH_{C\beta}$), 11.44 (br s, 0.72H, $NH_{B\beta}$), 11.68 (br s, 0.28H, $NH_{C\alpha}$), 7.36 (br s, 0.72H, $H_A{}^5{}_\beta$), 7.32 (s, 0.28H, $H_{X\alpha}$), 7.27−7.25 (m, 0.28H, $H_A{}^5{}_\alpha$), 7.23 (br s, 0.72H, $H_A{}^3{}_\beta$), 7.08 (s, 0.72H, $H_{X\beta}$), 7.01−7.00 (m, 0.28H, $H_A{}^3{}_\alpha$), 6.78 (s, 0.28H, $H_B{}^3{}_\alpha$), 6.70 (s, 0.72H, $H_B{}^3{}_\beta$), 6.42−6.40 (m, 0.72H, $H_A{}^4{}_\beta$), 6.36−6.34 (m, 0.28H, $H_A{}^4{}_\alpha$), 4.15 (s, 0.84H, $(OCH_3)_B{}^4{}_\alpha$), 4.02 (s, 2.16 H, $(OCH_3)_B{}^4{}_\beta$), 2.42−2.47 (m, 5H, $(CH_3)_C{}^5{}_{\alpha\beta}$, $(CH_2)_C{}^4{}_{\alpha\beta}$) 2.33 (s, 3H, CH_3SO_3), 2.21 (s, 0.84H, $(CH_3)_C{}^3{}_\alpha$), 2.19 (s, 2.16H, $(CH_3)_C{}^3{}_\beta$), 1.01 (t, J = 7.5 Hz, 3H, $(CH_3)_C{}^4{}_{\alpha\beta}$).

^{13}CNMR (DMSO-d_6, 100 MHz) of **1**·$MeSO_3H$ δ ppm 166.5 (Cq_β), 161.4 (Cq_α), 148.0 (Cq_β), 147.0 (Cq_β), 146.6 (Cq_α), 144.3 (Cq_α), 138.5 (Cq_α), 138.3 (Cq_α), 129.7 (Cq_α), 129.1 (Cq_β), 127.6 (CH_β), 126.5 (Cq_α), 126.2 (Cq_α), 125.1 (Cq_β), 122.6 (Cq_β), 121.7 (Cq_α), 121.0 (Cq_β), 119.7 (CH_α), 116.3 (CH_β), 114.1 (CH_β), 113.8 (CH_α), 112.6 (CH_β), 112.3 (CH_α), 96.1 (CH_α), 94.8 (CH_β), 60.7 ($(OCH_3)_B{}^4{}_\alpha$), 59.9 ($(OCH_3)_B{}^4{}_\beta$), 17.5 ($(CH_2)_C{}^4{}_\alpha$), 17.3 ($(CH_2)_C{}^4{}_\beta$), 15.4 ($(CH_3)_C{}^4{}_\beta$), 15.3 ($(CH_3)_C{}^4{}_\alpha$), 13.2 ($(CH_3)_C{}^5{}_\alpha$), 12.9 ($(CH_3)_C{}^5{}_\beta$), 10.1 ($(CH_3)_C{}^3{}_{\alpha\beta}$).

(Z)-2-(2-((1H-Pyrrol-2-yl)methylene)-3-methoxy-2H-pyrrol-5-yl)-1H-pyrrole **1**. 0.050 g (0.15 mol) of **1**.HCl were dissolved in CH_2Cl_2 (20 mL). This solution was treated with 30 mL of an aqueous NaOH solution 1%. The color changed from deep red to orange. The organic phase was dried with anhydrous Na_2SO_4 and the solvent removed. Compound **1** (0.041 g, 92%) was obtained as an orange solid. ^{1}HNMR ($CDCl_3$, 400 MHz, 25 °C) δ ppm 6.90 (s, 1H, H_x), 6.63 (dd, J = 3.5, 1.0 Hz, 1H, $H_A{}^3$), 6.58 (br s, 1H, $H_A{}^5$), 6.10 (dd, J = 3.5, 2.7 Hz, 1H, $H_A{}^4$), 6.07 (s, 1H, $H_B{}^3$), 3.96 (s, 3H, $(OCH_3)_B{}^4$), 2.23 (q, J = 7.5 Hz, 2H, $(CH_2)_C{}^4$), 2.11 (s, 3H, $(CH_3)_C{}^3$), 1.70 (s, 3H, $(CH_3)_C{}^5$), 0.95 (q, J = 7.5 Hz, 3H, $(CH_3)_C{}^4$). ^{13}CNMR ($CDCl_3$, 100 MHz) δppm 168.8, 158.7, 137.0, 129.7, 129.0, 125.7, 124.5, 122.6, 113.6, 111.9, 109.8, 95.4, 58.5, 17.5, 15.3, 10.2, 9.7. ^{1}H NMR ($CDCl_3$, 400 MHz, −50 °C) δ ppm12.65 (s, 1H, NH_A), 11.10 (s, 1H, NH_C), 6.87 (s, 1H, H_x), 6.63 (br s, 1H, $H_A{}^3$), 6.55 (br s, 1H, $H_A{}^5$), 6.12 (s, 1H, $H_B{}^3$), 6.08 (br s, 1H, $H_A{}^4$), 3.98 (s, 3H, $(OCH_3)_B{}^4$), 2.17 (q, J = 7.3 Hz, 2H, $(CH_2)_C{}^4$), 2.07 (s, 3H, $(CH_3)_C{}^3$), 1.54 (s, 3H, $(CH_3)_C{}^5$), 0.90 (q, J = 7.3 Hz, 3H, $(CH_3)_C{}^4$). ^{1}H NMR (DMSO-d_6, 400 MHz) δ ppm 11.66 (br s, 2H, NH_A, NH_C), 7.03 (dd, J = 2.2, 1.2 Hz, 1H, $H_A{}^5$), 6.66 (d, J = 2.5 Hz, 1H, $H_A{}^3$), 6.61 (s, 1H, H_X), 6.18 (dd, J = 3.5, 2.5 Hz, 1H, $H_A{}^4$), 6.08 (s, 1H, $H_B{}^3$), 3.82 (s, 3H, $(OCH_3)_B{}^4$), 2.33 (q, J = 7.5 Hz, 2H, $(CH_2)_C{}^4$), 2.32 (s, 3H, $(CH_3)_C{}^5$), 2.06 (s, 3H, $(CH_3)_C{}^3$), 0.99 (q, J = 7.5 Hz, 3H, $(CH_3)_C{}^4$).

HRMS (EI) m/z calcd for $[C_{18}H_{21}N_3O]$ 295.1679; found: 295.1685.

Computational Methods. The geometries of the complexes studied in this report were optimized without any symmetry constrains. In these calculations we used the BP86 density functional[26,27] in conjunction with the Ahlrichs quadruple-ζ plus polarization (def2-QZVP) basis sets[28] for all atoms. The reported BP86 calculations were carried out at the resolution of the identity (RI) level. Therefore, we have used the parallel RI-DFT methodology,[29,30] which uses an auxiliary fitting basis[31] to avoid treating the complete set of two-electron repulsion integrals, thus speeding up calculations significantly. We computed the interaction energy for each complex by subtracting the total energy of the optimized reference monomers from the total energy of the complex in the optimized geometry. The environment effects (with water as solvent) were taken into account by the COSMO[32] continuum solvation model. For all compounds we have carried out geometry optimization in water at the RI-BP86/def2-QZVP level. All calculations were performed using the TURBOMOLE program version 6.1.[33]

ASSOCIATED CONTENT

Supporting Information

NMR spectra (^{1}H, ^{13}C, COSY, NOESY) of compounds **1**, **1**·HCl, **1**·$MeSO_3H$, anion binding titration experiments, crystal data for **1**·HCl, **1**·$MeSO_3H$, absolute energies and Cartesian atom coordinates for all compounds. This material is available free of charge via the Internet at http://pubs.acs.org.

AUTHOR INFORMATION

Corresponding Author

*david.quinonero@uib.es; rquesada@ubu.es

Notes

The authors declare no competing financial interest.

ACKNOWLEDGMENTS

The authors thank financial support from Consejería de Educación de la Junta de Castilla y León (project

BU005B09) and the MICINN of Spain (CTQ2009-12631-BQU CTQ2011-27512/BQU and CTQ2009-14266-C02-02 projects, FEDER funds). We thank CONSOLIDER−Ingenio 2010 (CSD2010-0065) and the CESCA for computational facilities. D.Q. and R.Q. thank the MINECO of Spain for a "Ramón y Cajal" contract. We also thank Diego Aparicio for contributions to the synthesis of the reported compounds and Marta Mansilla and Dr. Jacinto Delgado (SCAI-Universidad de Burgos) for the X-ray determinations.

REFERENCES

(1) Fürstner, A. *Angew. Chem., Int. Ed.* **2003**, *42*, 308.
(2) Melvin, M. S.; Calcutt, M. W.; Noftle, R. E.; Manderville, R. A. *Chem. Res. Toxicol.* **2002**, *15*, 742.
(3) Pérez-Tomás, R.; Montaner, B.; Llagostera, E.; Soto-Cerrato, V. *Biochem. Pharmacol.* **2003**, *66*, 1447.
(4) Williamson, N. R.; Fineran, P. C.; Leeper, F. J.; Salmond, G. P. C. *Nat. Rev. Microbiol.* **2006**, *4*, 887.
(5) Williamson, N. R.; Fineran, P. C.; Gristwood, T.; Chawrai, S. R.; Leeper, F. J.; Salmond, G. P. C. *Future Microbiol.* **2007**, *2*, 605.
(6) Pandey, R.; Chander, R.; Sainis, K. B. *Curr. Pharm. Des.* **2009**, *15*, 732.
(7) Pérez-Tomás, R.; Viñas, M. *Curr. Med. Chem.* **2010**, *17*, 2222.
(8) Papireddy, K.; Smilkstein, M.; Kelly, J. X.; Shweta; Salem, S. M.; Alhamadsheh, M.; Haynes, S. W.; Challis, G. L.; Reynolds, K. A. *J. Med. Chem.* **2011**, *54*, 5296.
(9) Nguyen, M.; Marcellus, R. C.; Roulston, A.; Watson, M.; Serfass, L.; Madiraju, S. R. M.; Goulet, D.; Viallet, J.; Bélec, L.; Billot, X.; Acoca, S.; Purisima, E.; Wiegmans, A.; Cluse, L.; Johnstone, R. W.; Beauparlant, P.; Shore, G. C. *Proc. Natl. Acad. Sci. U.S.A.* **2007**, *104*, 19512.
(10) Davis, J. T. *Top. Heterocycl. Chem.* **2010**, *24*, 145.
(11) Hu, D. X.; Clift, M. D.; Lazarski, K. E.; Thomson, R. J. *J. Am. Chem. Soc.* **2011**, *133*, 1799.
(12) Haynes, S. W.; Sydor, P. K.; Corre, C.; Song, L.; Challis, G. L. *J. Am. Chem. Soc.* **2011**, *133*, 1793.
(13) Sertan-de Guzman, A. A.; Predicala, R. Z.; Bernardo, E. B.; Neilan, B. A.; Elardo, S. P.; Mangalindan, G. C.; Tasdemir, D.; Ireland, C. M.; Barraquio, W. L.; Concepcion, G. P. *FEMS Microbiol. Lett.* **2007**, *277*, 188.
(14) Falk, H.; Stressler, G.; Müller, N. *Monatsh. Chem.* **1988**, *119*, 505.
(15) Chen, K.; Rannulu, N. S.; Cai, Y.; Lane, P.; Liebl, A. L.; Rees, B. B.; Corre, C.; Challis, G. L.; Cole, R. B. *J. Am. Soc. Mass Spectrom.* **2008**, *19*, 1856.
(16) Díaz de Greñu, B.; Iglesias Hernández, P.; Espona, M.; Quiñonero, D.; Light, M. E.; Torroba, T.; Pérez Tomás, R.; Quesada, R. *Chem.—Eur. J.* **2011**, *17*, 14074.
(17) Konopleva, M.; Watt, J.; Contractor, R.; Tsao, T.; Harris, D.; Estrov, Z.; Bornmann, W.; Kantarjian, H.; Viallet, J.; Samudio, I.; Andreeff, M. *Cancer Res.* **2008**, *68*, 3413.
(18) Acoca, S.; Cui, Q.; Shore, G. C.; Purisima, E. O. *Proteins* **2011**, *79*, 2624.
(19) Espona-Fiedler, M.; Soto-Cerrato, V.; Hosseini, A.; Lizcano, J. M.; Guallart, V.; Quesada, R.; Pérez Tomás, R. *Biochem. Pharmacol.* **2012**, *83*, 489.
(20) Rizzo, V.; Morelli, A.; Pinciroli, V.; Sciangula, D.; D'Alessio, R. *J. Pharm. Sci.* **1999**, *88*, 73.
(21) Hynes, M. J. *J. Chem. Soc., Dalton Trans.* **1993**, 311.
(22) Jenkins, S.; Incarvito, C. D.; Parr, J.; Wasserman, H. H. *CrystEngComm* **2009**, *11*, 242.
(23) Cohen, Y.; Avram, L.; Frish, L. *Angew. Chem., Int. Ed.* **2005**, *44*, 520−554.
(24) Macchioni, A.; Ciancaleoni, G.; Zuccaccia, C.; Zuccaccia, D. *Chem. Soc. Rev.* **2008**, *37*, 479−489.
(25) Dairi, K.; Tripathy, S.; Attardo, G.; Lavallée, J.-F. *Tetrahedron Lett.* **2006**, *47*, 2605.
(26) Becke, A. D. *Phys. Rev. A* **1988**, *38*, 3098.
(27) Perdew, J. P. *Phys. Rev. B* **1986**, *33*, 8822.
(28) Weigend, F.; Ahlrichs, R. *Phys. Chem. Chem. Phys.* **2005**, *7*, 3297−3305.
(29) Eichkorn, K.; Treutler, O.; Öhm, H.; Häser, M.; Ahlrichs, R. *Chem. Phys. Lett.* **1995**, *242*, 652.
(30) Arnim, M. v.; Ahlrichs, R. *J. Comput. Chem.* **1998**, *19*, 1746.
(31) Weigend, F. *Phys. Chem. Chem. Phys.* **2006**, *8*, 1057.
(32) Klamt, A.; Schürmann, G. *J. Chem. Soc., Perkin Trans. 2* **1993**, 799.
(33) TURBOMOLE V6.1 2009, a development of University of Karlsruhe and Forschungszentrum Karlsruhe GmbH, 1989−2007, TURBOMOLE GmbH, since 2007; available from http://www.turbomole.com.